



AFRL-RY-HS-TR-2010-0015

A Velocity Profile Approximation for the Inner Region of the Turbulent Boundary Layer in an Adverse Pressure Gradient

David W. Weyburne

AFRL/RYHC
80 Scott Drive
Hanscom AFB, MA 01731-2909

10 September 2009

In-House Technical Report

APPROVED FOR PUBLIC RELEASE; DISTRIBUTION UNLIMITED

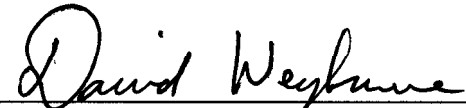
AIR FORCE RESEARCH LABORATORY
Sensors Directorate
Electromagnetics Technology Division
Hanscom AFB MA 01731-2909

NOTICE AND SIGNATURE PAGE

Using Government drawings, specifications, or other data included in this document for any purpose other than Government procurement does not in any way obligate the U.S. Government. The fact that the Government formulated or supplied the drawings, specifications, or other data does not license the holder or any other person or corporation; or convey any rights or permission to manufacture, use, or sell any patented invention that may relate to them.

This report was cleared for public release by the Electronic Systems Center Public Affairs Office for the Air Force Research Laboratory Electromagnetic Technology Division and is available to the general public, including foreign nationals. Copies may be obtained from the Defense Technical Information Center (DTIC) (<http://www.dtic.mil>).

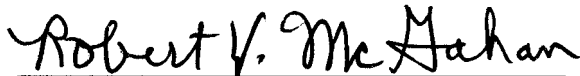
AFRL-RY-HS-TR-2010-0015 HAS BEEN REVIEWED AND IS APPROVED FOR PUBLICATION IN ACCORDANCE WITH ASSIGNED DISTRIBUTION STATEMENT.



DAVID WEYBURNE
Contract Monitor



DAVID F. BLISS, Acting Chief
Optoelectronic Technology Branch



ROBERT V. McGAHAN
Technical Communications Advisor
Electromagnetics Technology Division

This report is published in the interest of scientific and technical information exchange, and its publication does not constitute the Government's approval or disapproval of its ideas or findings.

REPORT DOCUMENTATION PAGE

Form Approved
OMB No. 0704-0188

Public reporting burden for this collection of information is estimated to average 1 hour per response, including the time for reviewing instructions, searching existing data sources, gathering and maintaining the data needed, and completing and reviewing this collection of information. Send comments regarding this burden estimate or any other aspect of this collection of information, including suggestions for reducing this burden to Department of Defense, Washington Headquarters Services, Directorate for Information Operations and Reports (0704-0188), 1215 Jefferson Davis Highway, Suite 1204, Arlington, VA 22202-4302. Respondents should be aware that notwithstanding any other provision of law, no person shall be subject to any penalty for failing to comply with a collection of information if it does not display a currently valid OMB control number. PLEASE DO NOT RETURN YOUR FORM TO THE ABOVE ADDRESS.

1. REPORT DATE (DD-MM-YYYY) 10-09-2009	2. REPORT TYPE Technical Report	3. DATES COVERED (From - To) 1 Dec 2008 – 1 Sep 2009		
4. TITLE AND SUBTITLE A Velocity Profile Approximation for the Inner Region of the Turbulent Boundary Layer in an Adverse Pressure Gradient		5a. CONTRACT NUMBER In-House		
		5b. GRANT NUMBER		
		5c. PROGRAM ELEMENT NUMBER 624916		
6. AUTHOR(S) David W. Weyburne		5d. PROJECT NUMBER 4916		
		5e. TASK NUMBER HC		
		5f. WORK UNIT NUMBER 01		
7. PERFORMING ORGANIZATION NAME(S) AND ADDRESS(ES) AFRL/RYHC 80 Scott Drive Hanscom AFB, MA 01731-2909		8. PERFORMING ORGANIZATION REPORT NUMBER		
9. SPONSORING / MONITORING AGENCY NAME(S) AND ADDRESS(ES) Electromagnetics Technology Division Sensors Directorate Air Force Research Laboratory 80 Scott Drive Hanscom AFB, MA 01731-2909 Source Code: 437890		10. SPONSOR/MONITOR'S ACRONYM(S) AFRL/RYHC		
		11. SPONSOR/MONITOR'S REPORT NUMBER(S) AFRL-RY-HS-TR-2010-0015		
12. DISTRIBUTION / AVAILABILITY STATEMENT DISTRIBUTION A: APPROVED FOR PUBLIC RELEASE: DISTRIBUTION UNLIMITED				
13. SUPPLEMENTARY NOTES The U.S. Government is joint author of this work and has the right to use, modify, reproduce, release, perform, display, or disclose the work. Cleared for Public Release by 66ABW-2010- , date				
14. ABSTRACT A new near-wall approximate analytical velocity profile is developed for wall-bounded turbulent boundary layers in an adverse pressure gradient. The new velocity profile approximation is used to fit experimental profile data in order to extract near-wall information such as the skin friction coefficient and the viscous layer thickness. Results with Direct Numerical Simulation computer generated data shows the method works well and is superior to the existing model from the literature. Fits to experimental wind tunnel APG data sets indicate that the new analytical velocity profile works well.				
15. SUBJECT TERMS Fluid Boundary Layers, Velocity Profiles, Turbulent Flow, Adverse Pressure Gradient				
16. SECURITY CLASSIFICATION OF: a. REPORT Unclassified		17. LIMITATION OF ABSTRACT SAR	18. NUMBER OF PAGES 26	19a. NAME OF RESPONSIBLE PERSON David W. Weyburne
b. ABSTRACT Unclassified				19b. TELEPHONE NUMBER n/a
Standard Form 298 (Rev. 8-98) Prescribed by ANSI Std. Z39.18				

Contents

List of Figures	iv
Acknowledgments	vi
Summary	1
1. Introduction	2
2. Approximate Turbulent Velocity Profile	3
3. Flows with a Pressure Gradient	4
4. Experimental DNS Results	5
5. Experimental Fitting Results	7
6. Discussion	9
7. Conclusion	13
References	14
Appendix A	16

List of Figures

Figure 1. The crosses connected by the black lines are the ZPG DNS results from Spalart [5] at $R_* = 2000$	6
Figure 2. The crosses connected by the black lines are the ZPG DNS results from Khujadze and Oberlack [6] with $R = 2807.098$	6
Figure 3. The crosses connected by the black lines are the ZPG DNS results from Hoyas and Jimenez [7] at $R = 2000$	6
Figure 4. The crosses connected by the black lines are the ZPG DNS results from Komminaho and Skote [8] at $R_* = 450$	6
Figure 5. The crosses connected by the black lines are the APG DNS results from Lee and Sung [11] at the reduced pressure $\epsilon = 1.68$	8
Figure 6. The crosses connected by the black lines are the APG DNS results from Komminaho and Skote [8] at the reduced pressure $P^+ = 0.01791$	8
Figure 7. The crosses connected by the black lines are the APG DNS results from Skote and Henningson [12] at the reduced pressure $P^+ = 0.05435$	8
Figure 8. The crosses connected by the black lines are the APG DNS results from Skote and Henningson [12] at the reduced pressure $P^+ = 0.07093$	8
Figure 9. The crosses connected by the black lines are the experimental APG results from Nagano, Tagawa, and Tsuji [13].	9
Figure 10. The crosses connected by the black lines are the experimental APG results from Skåre and Krogstad [14] at $x = 4.0\text{m}$ and $x = 5.2\text{m}$	9
Figure 11. The black line is the second derivative of the Blasius solution for laminar flow using the Schlichting [19] tabulated values.	12

Acknowledgement

The author would like to acknowledge the support of the Electromagnetics Technology Division of the Sensors Directorate of the Air Force Research Laboratory. In addition, the author would like to thank a number of authors who contributed their experimental datasets including Philippe Spalart, George Khujadze and Martin Oberlack, Jukka Komminaho and Martin Skote, Y. Nagano, M. Tagawa and T. Tsuji, Javier Jimenez and Sergio Hoyas, Joung-Ho Lee and Hyung Jin Sung, Martin Skote and Dan Henningson, and Per Egil Skåre and Per-Åge Krogstad.

Summary

A new near-wall approximate analytical velocity profile is developed for wall-bounded turbulent boundary layers in an adverse pressure gradient. The new velocity profile approximation is used to fit experimental profile data in order to extract near-wall information such as the skin friction coefficient and the viscous layer thickness. Results with Direct Numerical Simulation computer generated data shows the method works well and is superior to the existing model from the literature. Fits to experimental wind tunnel APG data sets indicate that the new analytical velocity profile works well.

1. Introduction

It has long been recognized that the wall-bounded turbulent boundary layer can be conveniently divided into two regions, an inner and outer region. The proximity of the wall has made experimental measurements very difficult in the inner layer region. This, in turn, has made it very difficult to extract information such as the skin friction coefficient and the thickness of the viscous layer. The usual method for extracting the skin friction coefficient from velocity profile data is to use the Clauser chart method or its equivalent. This method basically assumes the Logarithmic Law of the Wall. Although there is an on-going controversy as to the universality of the Logarithm Law [1], the Clauser method is the only available option for most engineering purposes. Recently, Kendall and Koochesfahani [2] described a related method for estimating the turbulent boundary layer skin friction coefficient of a zero pressure gradient (ZPG) flow. The method is based on fitting the experimental inner region velocity profile. While still assuming the Log Law, the method also makes use of data close to the wall. Kendall and Koochesfahani found that fits using the approximate Musker velocity profile [3] gave skin friction coefficients that were very close to experimentally verified oil-film interferometry results. The Musker profile equation is a simple analytical equation that tries to describe the velocity profile from the wall to the outer reaches of the Log Law region.

The fitting method works very well for the ZPG turbulent boundary layer. Unfortunately, it is not applicable to flows with an adverse pressure gradient (APG). The reason is that it is generally acknowledged that the Karmon constant κ , which is central to the Log Law, has an unknown pressure gradient dependence. Recently, T. Nickels [4] presented a simple analytical model for the velocity profile for the inner region of the APG boundary layer that includes for the first time a simple pressure dependent parameter developed from fitting Direct Numerical Simulation (DNS) computer generated datasets. With the Nickels model, it would be possible to fit APG velocity profiles and thereby extract skin friction coefficients and viscous thicknesses. In what follows, we compare the Nickels analytical expression to more recent DNS results. We find that the Nickels expression works well for the ZPG case and mild APG case. However, for the strong APG case, the Nickels expression does not reproduce the velocity profile nearly as well. To address this problem, we looked for alternate approximate velocity profile expressions that would fit the data better.

Rather than trying to find alternative approximate velocity profiles directly, we opted to look for approximate second derivative profiles. The reason for this approach is two-fold. First, the pressure gradient contribution to the velocity profile shows up directly as a wall boundary condition to the second derivative velocity profile. From the streamwise momentum balance, we know that at the wall, the derivative of the pressure in the streamwise direction is directly balanced by the viscous second derivative (normal to the wall direction) term. The derivative of the pressure in the streamwise direction is a value easily measured experimentally. Thus, using the second derivative profile, it is much easier to see the effect of the pressure gradient on the boundary layer profile. The second reason for using this approach is that by working with the second derivative profile, we can see exactly where the viscous contributions are important. The viscous forces are one of the major forces controlling the inner region of the boundary layer.

It must be pointed out that although we are developing a second derivative velocity profile, the intent is to end up with an approximate velocity profile since the velocity profile is what is measured experimentally. Therefore, an overriding requirement is that any second derivative analytical approximation must be twice integrable in order to obtain a workable velocity profile approximation.

After testing various analytical expressions for the second derivative profiles against a number of DNS experimental results, we found that a simple delta-function-like analytical expression for the pressure contribution together with the differentiated Musker profile reproduced the second derivative experimental profiles very well. In what follows, we begin by introducing the Musker profile for the ZPG case. For comparison, we also present the Nickels expression. Next we introduce the simple delta-function-like expression for the pressure contribution. Comparisons to experimental DNS results show that the new expression is superior to the Nickels approximate expression for the turbulent boundary layer in an adverse pressure gradient. Finally, the new modified Musker profile is used to fit existing APG data with good results.

2. Approximate Turbulent Velocity Profile

The velocity profile for a turbulent fluid flow past a flat plate developed by Musker [3] is based on an eddy kinematic viscosity argument as to the form of the reduced velocity gradient. In the paper, Musker showed that the reduced velocity gradient is given approximately as

$$\frac{du^+}{dy^+} \approx \frac{+C(y^+)^2}{+C(y^+)^2 + C(y^+)^3} \quad (1)$$

where $u^+ = u/u$, where $y^+ = y u^+ / \tau_w$, and where u^+ is the friction velocity. In this equation the constant τ_w is the well-known Log Law von Karman constant and C is proportionality constant for the eddy viscosity in the near-wall region. Musker estimated the value of C by matching the integral of Eq. 1 and the Log Law velocity for large y^+ values.

To calculate the velocity profile, we need to integrate Eq. 1. Although a general closed form analytical integration of Eq. 1 is not possible, it is possible to analytically integrate Eq. 1 for specific numerical values of C and τ_w . For example, Musker showed that for the values $C=0.001093$ and $\tau_w = 0.41$, the analytical velocity profile derivative (Eq. 1) integrates to

$$u_{Musker}^+ = 5.424 \tan^{-1} \left[\frac{(2y^+ - 8.15)}{16.7} \right] + \log_{10} \left[\frac{(y^+ + 10.6)^{9.6}}{(y^{+2} - 8.15y^+ + 86)^2} \right] - 3.52 \quad (2)$$

This equation works very well for the zero pressure gradient (ZPG) turbulent boundary layer as shown by A. Kendall and M. Koochesfahani [2]. For the general C and τ_w case, we prefer the approximate integral expression given as FORTRAN source code in Appendix A. The advantage of the expression given in Appendix A is that it is applicable for flows with a pressure gradient since the values of both C and τ_w are expected to change with the strength of the pressure gradient.

3. Flows with a Pressure Gradient

If Eq. 1 is differentiated with respect y^+ then one has

$$\frac{d^2 u_{Musker}^+}{dy^{+2}} = \frac{-C(y^+)^2(3 + C(y^+)^2)}{(1 + C(y^+)^2 + C(y^+)^3)^2} \quad (3)$$

Notice that at the wall, this equation has a value of zero. The momentum balance equation in the direction parallel to the wall simplifies at the wall to

$$\frac{1}{dx} \frac{dp}{dx} \equiv \frac{d^2 u}{dy^2} \quad (4)$$

Therefore for the zero pressure gradient (ZPG) case we must have the second derivative of the velocity be equal to zero in agreement with Eq. 3. The question is what to do for the case with a non-zero pressure gradient.

Recently, Nickels constructed an analytical model to handle the strong APG case [4]. The Nickels expression is a composite of three different expressions covering different regions of the boundary layer. For the inner viscous region, Nickels found that the analytical expression given by

$$u^+|_{viscous} = y_c^+ \left(1 - \left(1 + 2 \left(y^+ / y_c^+ \right) + \frac{1}{2} \left(3 - p_x^+ y_c^+ \right) \left(y^+ / y_c^+ \right)^2 - \frac{3}{2} p_x^+ y_c^+ \left(y^+ / y_c^+ \right)^3 \right) e^{-3y^+ / y_c^+} \right) \quad (5)$$

was a good fit to a number of DNS experimental results. In this expression, the only adjustable parameter is y_c^+ whose value as a function of the pressure gradient was found by fitting DNS data. For the Overlap region, Nickels choose a mixed scale function involving the inner region scale as well as the outer region scale. The function was chosen to have the correct asymptotic behavior and is given by

$$u^+|_{overlap} = \frac{1}{6} \ln \left(\frac{1 + (0.6(y^+ / y_c^+))^6}{1 + (y^+ /)^6} \right) \quad (6)$$

where $$ is a boundary layer thickness scale treated as an adjustable parameter. The final expression of Nickels composite expression for the velocity profile covers the wake region. It is given by

$$u^+|_{wake} = b \left(1 - \text{EXP} \left(\frac{5 \left(\frac{4}{y_c^+} + \frac{8}{y^+} \right)}{1 + 5^3} \right) \right) \quad (7)$$

where b is a measure of the wake strength. By fitting to DNS datasets, Nickels was able to find simply analytical expressions for y_c^+ and $$ as a function of the pressure gradient. This means that the only unknown parameters are u , b , and $$ which are obtained by fitting the composite profile (Eqs. 5-7) to the experimental profile.

The Nickels expressions work well for the ZPG case and mild pressure gradient cases. Unfortunately, as we will show below, it does not work nearly as well for the medium and strong APG cases. To remedy this problem, we looked for an improved analytical expression that followed the experimental data better. We found that adding a

simple delta-function-like expression to the standard Musker analytical expression given in Appendix A works very well. The delta-function-like expression was chosen so that the resulting composite velocity profile has the correct Taylor series expansion at the wall. The delta-function-like expression is given by

$$\frac{d^2 u^+}{dy^{+2}} \bigg|_{\text{delta}} = \frac{dP}{dx} e^{-a(y^+)^2} \left(1 - 2a(y^+)^2 \right) \quad (8)$$

where a is a constant determined from comparison with DNS experimental results. For the work described herein, a value of $a = 0.1$ was found to work well. If Eq. 8 is twice integrated using the appropriate boundary conditions, then we obtain

$$u^+ \bigg|_{\text{delta}} = \frac{1}{2a} \frac{dP}{dx} \left(1 - e^{-a(y^+)^2} \right) \quad (9)$$

Therefore, the velocity profile that we found that works well is given by a combination of the Musker velocity profile (Appendix A) together with Eq. 9 and will be henceforth designated as the modified Musker profile.

4. Experimental DNS Results

In order to understand the nature of the problem, it is advantageous to look at examples of second derivative profiles for turbulent boundary layer flows. Since it is not possible to calculate turbulent velocity profiles theoretically, our only recourse is to look at experimental data. However, most of the available datasets for turbulent velocity profiles with pressure gradients, suffer from two problems. The first problem is that near-wall measurements are very difficult to perform and the second is that in general, it is very difficult to numerically differentiate velocity profile data reliably in the presence of experimental noise.

One way to overcome both of these problems is to use computer generated Direct Numerical Simulation (DNS) experimental results. The numerical nature of this path makes it straightforward to calculate the second derivative profile. We begin by looking at the ZPG case. In Figs. 1-4 we show experimental DNS data from a number of sources. In Fig. 1, for example, we show the $Re_* = 2000$ DNS dataset from Spalart [5] as crosses connected by black lines. The red lines in all of the figures are the Nickels result using the values of y_c^+ and $p_x^+ = 0$ advocated by Nickels [4] and then fitting for the parameters u , b , and C . The blue line in all of these figures are the Musker results obtained by fitting u , C , and b . It is readily apparent that both the Nickels and the modified Musker profile work well for the ZPG case.

In all of these figures, the viscous layer thickness scaling variable is the moment based mean location of the boundary layer given by δ_1 and defined as

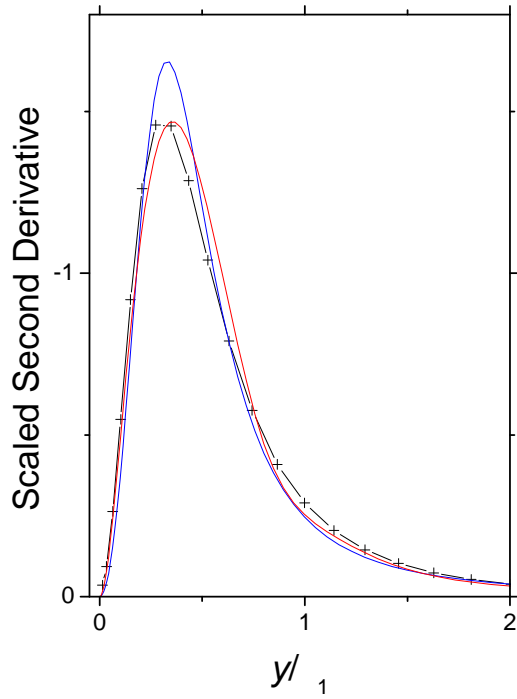


Figure 1: The crosses-black lines are from Spalart [5] at $R_* = 2000$.

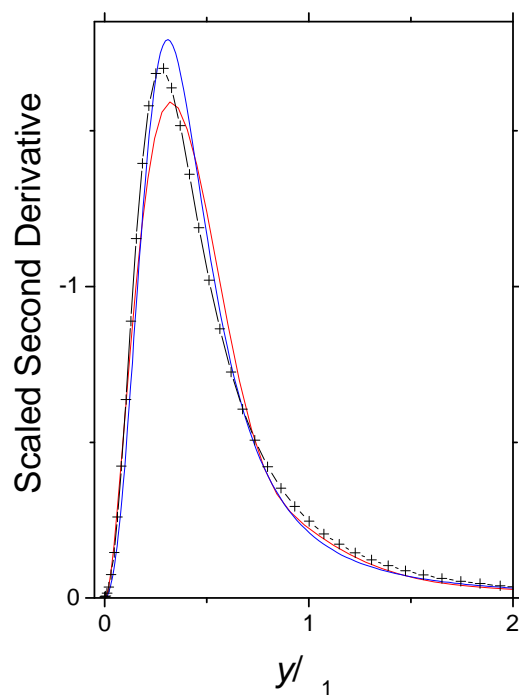


Figure 2: The crosses-black lines are Khujadze and Oberlack [6] at $R = 280$.

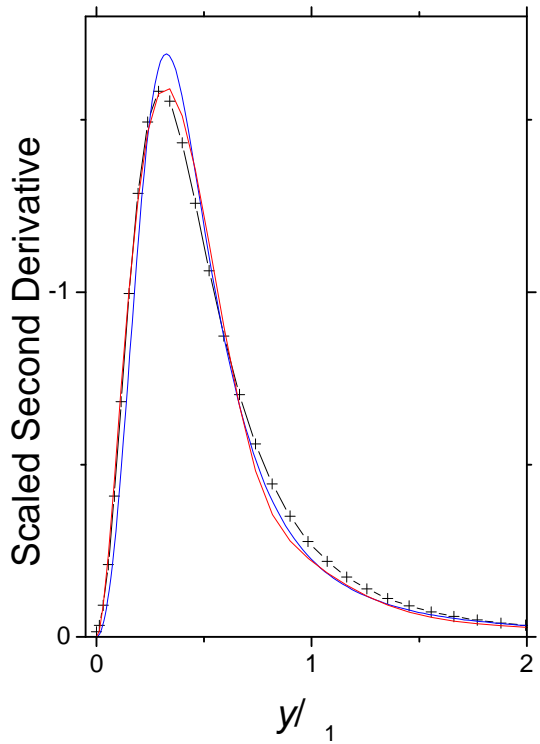


Figure 3: The crosses-black lines are Hoyas and Jimenez [7] at $R = 2000$.

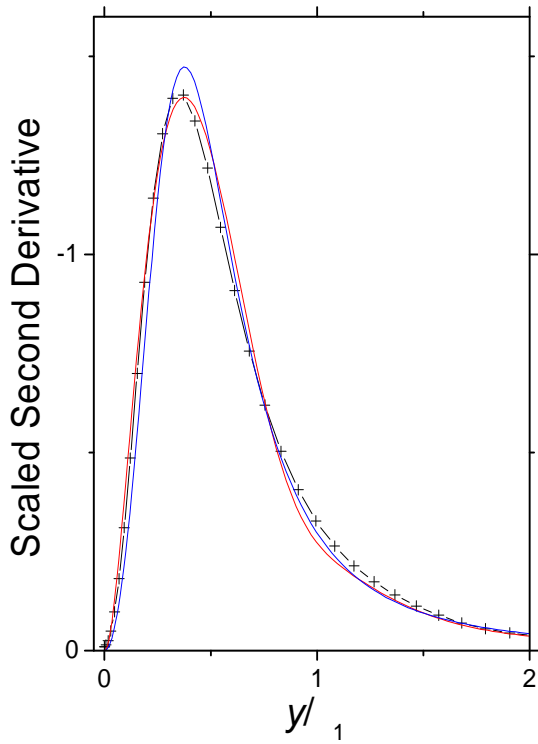


Figure 4: The crosses-black lines are Komminaho and Skote [8] at $R_* = 450$.

$$\frac{u_e}{1} = \frac{du(y)}{dy} \Big|_{y=0} \quad (10)$$

where u_e is the free stream velocity. This parameter is one of a number of new thickness and shape parameters developed by Weyburne [9,10]. The new parameters are based on a probability distribution function methodology, where the boundary layer is described in terms of central moments of various Gaussian-like kernels based on the velocity profile or its first two derivatives [10]. The mean location \bar{y}_1 is the first moment about the origin of the second derivative profile. It is therefore appropriate to use \bar{y}_1 as the length scale for second derivative profiles.

Now let us examine the APG case. In Figs. 5-8 we show APG DNS data from a number of sources. In Fig. 5, for example, we show a DNS result of Lee and Sung [11] as crosses connected by black lines. Notice the behavior of the Nickels (red line) analytical profile in the region just to the right of the peak. The Nickels analytical expression is at first higher than the experimental result and then, at about half way down from the peak, drops lower than the experimental result. This same behavior occurred for the ZPG case but it becomes more exaggerated as the pressure gradient becomes larger. This is especially evident in the DNS results of Skote and Henningson [12] shown in Figs. 6-8. At the largest pressure gradients (Figs. 7 and 8), the Nickels analytical expression (red lines) is not following the experimental DNS results very well. The modified Musker profile (blue lines), in contrast, appears to fit the data for all cases very well.

The major objective of the present study is to present a method for extracting the skin friction coefficient c_f and the related viscous scaling length for turbulent boundary layers with an adverse pressure gradient. Of the ten APG DNS cases investigated, we found the average absolute deviation of the fitted c_f value from the reported value was 1.0% (calculated from the fitted and the reported u values using $c_f = 2u^2/u_e^2$). We believe this small error supports the notion that the modified Musker method is a valid technique for extracting the skin friction coefficient and the related viscous scaling length.

5. Experimental Fitting Results

Having established that the modified Musker profile (Appendix A together with Eq. 9) fits the DNS data very well, we now turn to the task of using this composite profile to extract skin friction coefficients and the viscous layer thickness from regular wind tunnel experimental results. As we have already pointed out, Kendall and Koochesfahani [2] have shown that the Musker profile fitting procedure works well for the ZPG case. The DNS results of Figs. 1-4 confirm this result. We therefore will emphasize the APG fitting results. In contrast to the ZPG case, there are not any APG datasets for which high precision independent measurements of the skin friction coefficient (e.g., oil interferometry) have been made available to this author. We therefore limit ourselves to showing plots of the fits to existing experimental data sets. In Fig. 9 we show four profiles reported by Nagano, Tagawa and Tsuji [13]. In Fig. 10 we

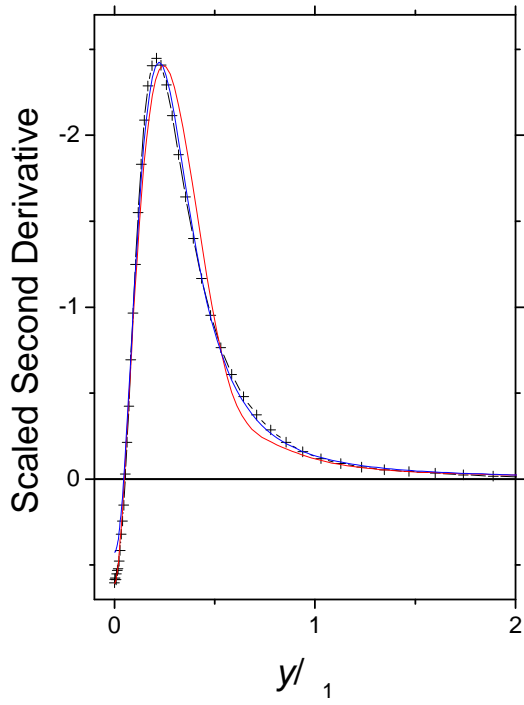


Figure 5: The crosses-black lines are Lee and Sung [9] at $\gamma = 1.68$.

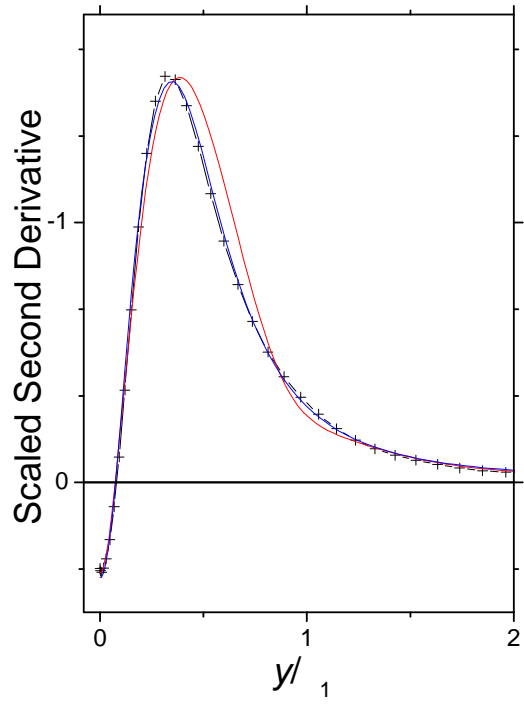


Figure 6: The crosses-black lines are Komminaho and Skote [8] at $P^+ = 0.01791$.

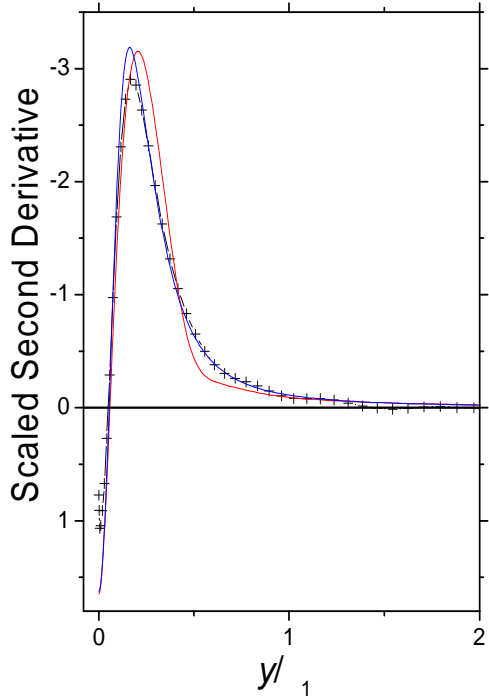


Figure 7: The crosses-black lines are Komminaho and Skote [8] at $P^+ = 0.05435$.

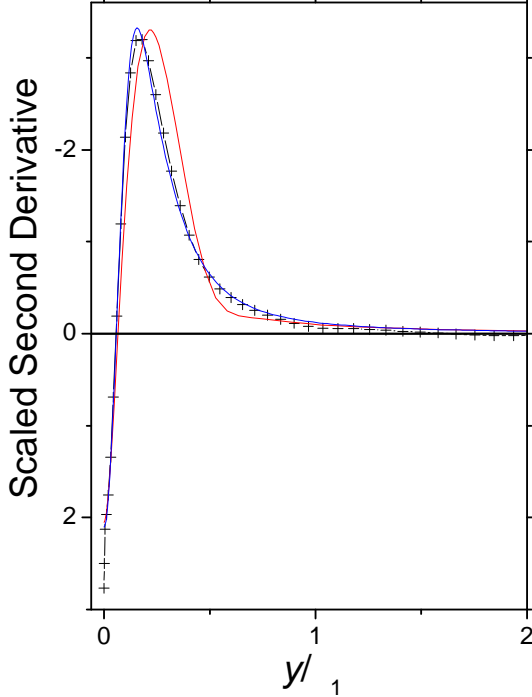


Figure 8: The crosses-black lines are Komminaho and Skote [8] at $P^+ = 0.071$.

show the fitting results for two of the seven profiles reported by Skåre and Krogstad [14]. In both cases the modified Musker fitted lines are displayed as blue lines. It is readily evident that the modified Musker equation is a good fit to the experimental data.

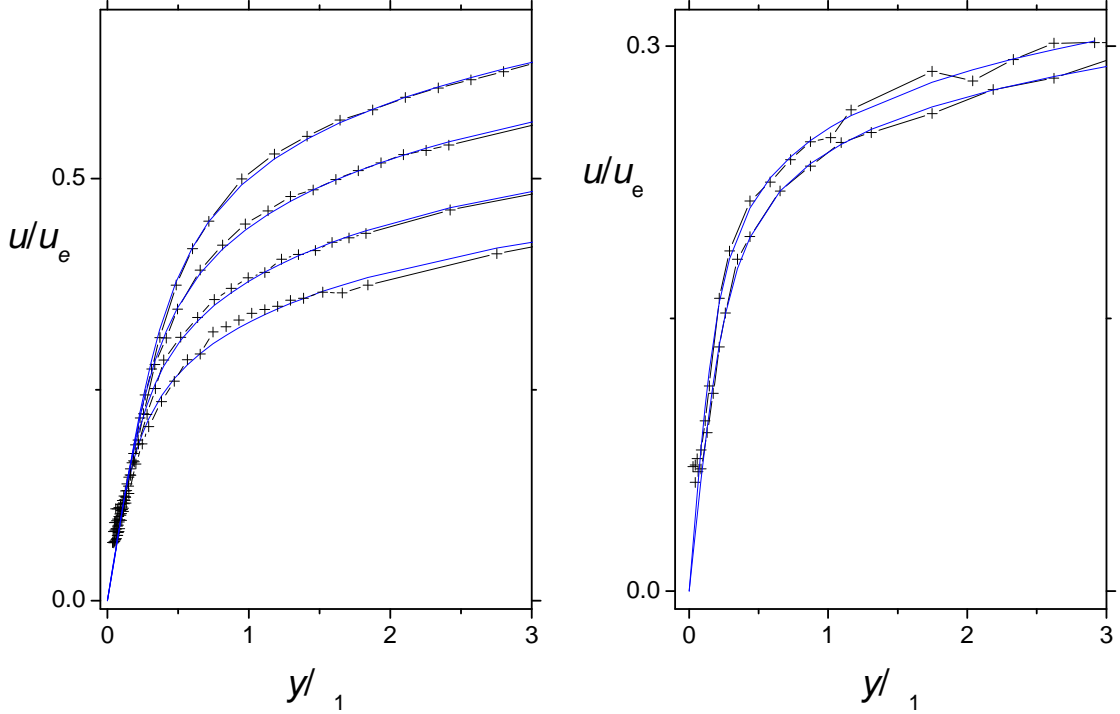


Figure 9: The crosses-black lines are Nagano, Tagawa and Tsuji [13] results.

Figure 10: The crosses-black lines are Skåre and Krogstad [14] APG results.

6. Discussion

The plotted results for Figs. 9 and 10 indicate that the modified Musker profile works well. The extracted skin friction coefficients are at worst within $\sim 22\%$ of the reported values from the authors reported values. Note that the reported methods used to measure the experimental skin friction coefficient are instructive. Nagano, Tagawa and Tsuji [13], for example, developed their own method for measuring the skin friction coefficient. It is based on the fact that the measured velocity profile values close to the wall have a noticeable systematic instrumental error. Their skin friction coefficient extraction method actually incorporates this instrumental error. Given the fact that the systematic instrumental error is probably not reproducible from wind tunnel to wind tunnel, this method has not been adopted by any other group to our knowledge.

In the other experimental APG case, Skåre and Krogstad [14] used a number of techniques to calculate the skin friction coefficient including a fitting method based on a composite profile that included the Musker [3] velocity profile. They provide few details of the model function but it is evident that they did not apply a correction for the fact that

the profiles were measured in an adverse pressure gradient. Skåre and Krogstad also used pilot tube measurements to estimate the skin friction coefficient. However, the pilot tube method assumes the Log Law is applicable and does not correct for pressure gradients. The two experimental results emphasize the fact that the presently available methods for extracting skin friction coefficient and viscous layer thickness for the APG case are not adequate.

The above experimental fitting results indicate that a fitting procedure utilizing the modified Musker velocity profile should be useful for extracting skin friction coefficients and viscous layer thicknesses for both the ZPG and APG cases. However, the parameter extraction is only useful in so far as the analytical function correctly approximates the behavior of the real turbulent boundary layer. It is therefore imperative to show that at some level the approximate profile has some theoretical underpins that would give some confidence in the extracted data values. As a first step we note that the boundary conditions at the wall for the modified Musker profile are correct for the velocity profile and its first two derivatives.

The next step was to look at the near wall behavior. The near wall behavior was investigated by looking at the Taylor Series expansion of the modified Musker profile. It is readily verified that the Taylor Series expansion of the modified Musker profile at the wall is given by

$$u^+ \equiv y^+ + \frac{1}{2} p^+ (y^+)^2 - \left[\frac{C}{4} + \frac{ap^+}{4} \right] (y^+)^4 + h.o.t. . \quad (11)$$

Note that for the ZPG case, this quartic dependence was obtained from theoretical considerations by Cenedese, Romano, and Antonia[15] as well as Park and Chung [16] and confirmed by the careful near-wall experimental results of Poggi, Porporato, and Ridolfi [17]. Using the Musker value for C , the quartic numerical coefficient in Eq. 11 is -0.00027 compared to the value of -0.00025 advocated by Park and Chung [16] for the ZPG case. The close agreement of the coefficients gives support to the modified Musker model.

The importance of the quartic term in Eq. 11 should not be under stated. In the region from $0 < y/ \delta_1 < 1$ (which corresponds to $0 < y^+ < 25$), the second derivative profiles and therefore the viscous contributions are significant (see Figs. 1-8). This is true even in the very near wall region ($0 < y/ \delta_1 < 0.2$ which corresponds to $0 < y^+ < 5$) where it is often assumed that the velocity profile is a linear function of the distance. The second derivative of a linear function is zero, which would mean there would be no viscosity contribution to the flow in this region. In fact the opposite is true, the viscosity contribution basically peaks at $y/ \delta_1 \sim 0.2$. Furthermore, it is evident from Figs. 1-8 that a linear profile does not exist in any of the DNS data sets that we have looked at. It is therefore important that the fluid flow community should replace any references to a linear velocity profile for the turbulent boundary layer with something more appropriate such as “almost linear”.

In the region where the Log Law is applicable, the modified Musker profile is expected to produce very similar fitting results compared to the traditional Log Law fits. For the ZPG case, as an example, the difference between the Log Law and the Musker profile was less than 0.1% for $y^+ = 100$ and the difference decreased as y^+ increased in

value. Since the Log Law behavior has been demonstrated in countless ZPG experimental data sets, then we should expect the modified Musker profile to produce similarly good fitting results at comparable distances from the wall. For the nonzero pressure gradient case, it is easily shown that the pressure gradient term given by Eq. 9 results in a constant value in the Log Law region. The net result is that in this region, the modified Musker profile follows the traditional Log Law behavior but with a different Karmon constant. This Log Law behavior for flows with pressure gradients is confirmed by the recent experimental results of Nagib, Christoperou, and Monkewitz [18].

We have just shown that the modified Musker profile has the correct wall boundary conditions, the correct near wall behavior, and similar behavior to the Log Law in the region where the Log Law is traditionally applicable. Together with the demonstrated excellent results for the DNS and experimental fits, these results indicate that the new modified Musker method should fit the actual near wall behavior of the turbulent boundary layer very well. The composite profile developed by Nickels also has many of these same properties. How does one explain the difference in the modified Musker and the Nickels profiles? We believe the major difference is in how the transition from the near-wall behavior to the logarithmic form is handled in the two methods. In the Nickels case the transition is handled as a simple sum of two separate approximate forms (the sum of Eqs. 6 and 7).

The Musker transition is handled differently. The Musker development is based on an eddy viscosity approach and, in the near wall area, Musker makes an argument for the eddy viscosity, τ_t , behaving as

$$\tau_t / \tau \approx C(y^+)^3. \quad (11)$$

In the Log law region it is known that $\tau_t / \tau \approx y^+$. To make the transition between the two regions smoothly, Musker employed the simple interpolation form

$$\frac{1}{\tau_t / \tau} \approx \frac{1}{C(y^+)^3} + \frac{1}{y^+}. \quad (12)$$

Using this value of the eddy viscosity, Musker then goes on to assume that the shear stress is constant so that we have

$$\left. \frac{\partial u}{\partial y} \right|_{y=0} \approx (+ \tau_t) \frac{\partial u}{\partial y}. \quad (13)$$

Substituting Eq. 12 into Eq. 13 and rearranging, it is easy to show that one obtains the Musker expression given by Eq. 1. Thus the Musker expression covers the same region as Nickels two separate approximate forms. The key difference is that the Musker transition is handled with an interpolation formula (Eq. 12) rather than as a simple sum as is the case for the Nickels method. The requirements for a smooth transition between two terms are much more demanding using a sum compared to an interpolation using Eq. 12. Therefore, the two term transition for Nickels model works well at zero and low pressure gradient values, but fails at higher pressure gradient values.

Having established the applicability of the modified Musker method for extracting the skin friction coefficient by fitting, we now turn to what information we can extract on the viscous layer region. First we note that from the skin friction coefficient it is possible to calculate τ_1 , the mean value of the scaled second derivative profile using Eq. 10. The

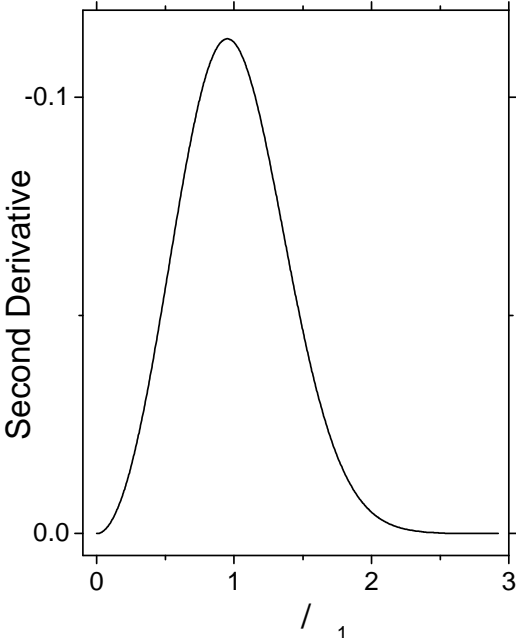


Figure 11: The second derivative of the Blasius solution using the Schlichting [19] tabulated values.

second derivative divided by the second central moment to the $3/2$ power [9,10]. For the Blasius solution to laminar flow, the skewness $\gamma_1 = 0.3$ whereas for the turbulent flow curve given in Fig. 1, for example, the value is $\gamma_1 = 7.8$ (for comparison, the skewness of a Gaussian curve is $\gamma_1 = 0$). We bring this up in order to emphasize what other researchers have pointed out; that for the turbulent boundary layer, the viscous forces have a significant presence in what is traditionally called the Buffer layer region.

One of the advantages of the modified Musker fitting method over the traditional Clauser method is that it is only necessary to choose one fitting limit for the Modified Musker method versus two fitting limits (lower and upper limit) for the Clauser method. For the modified Musker method the wall is one fitting limit. This means that it is only necessary to choose the upper fitting limit. In the fits used in this study, the upper fitting limit was chosen to be $y \sim 2.5 \gamma_1$. For the Clauser method it is necessary to choose a lower and upper fitting limit for where the Log Law is applicable. One of the major failings of those that advocate for the universality of the Log Law is that there is not a standard method for defining where the Log Law is applicable. This means that each practitioner is free to pick the lower and upper limits. The problem with this is that the velocity profile plotted in y -plus log units is an S-curve such that the linear Log line is in the middle. Thus, by simultaneously shrinking the lower limit and lengthening the upper limit (or vice versa), one can change the fitted linear line to take on a range of fitted parameters. With the modified Musker method, one can only change the upper limit. By starting out with a large upper limit and steadily shrinking the upper limit by one data point at a time, one will see that the fitted parameters will tend to converge to a specific value. Therefore, besides utilizing more data points, the Modified Musker method has

$y = \gamma_1$ location basically identifies the central location for the viscous forces. Notice in the turbulent flow DNS data (Figs. 1-8), the $y = \gamma_1$ location is shifted significantly to the right of the main peak. Compare these turbulent flow results with the “laminar” flow second derivative curve depicted in Fig. 11. Notice that for laminar flow the second derivative peaks near $y = \gamma_1$. It is evident that for turbulent flow, there are viscous contributions to the flow that do not originate from the flow-wall interaction. What this indicates is that the viscous force curves for turbulent flow are noticeably skewed compared to laminar flow. This fact is emphasized by looking at the skewness parameter γ_1 defined as the third central moment of the scaled

12

the advantage that the fitting parameters tend to converge to a specific set of values compared to the traditional Clauser method.

7. Conclusion

An approximate velocity profile for the turbulent boundary layer in an adverse pressure gradient was developed. The approximate profile was found to fit DNS as well as experimental wind tunnel datasets very well. The new approximate velocity profile was used to extract the skin friction coefficient and the viscous layers mean value location.

References

- [1] M. Buschmann, and M. Gad-el-Hak, "Recent developments in scaling of wall-bounded flows," *Prog. Aerospace Sci.*, vol. 42, 419(2007).
- [2] A. Kendall and M. Koochesfahani, "A method for estimating wall friction in turbulent wall-bounded flows," *Exp Fluids*, vol. 44, 773(2008).
- [3] A. Musker, "Explicit expression for the smooth wall velocity distribution in a turbulent layer," *AIAA J.*, vol. 17, 655(1979).
- [4] T. Nickels, "Inner scaling for wall-bounded flows subject to large pressure gradients," *J. Fluid Mech.*, vol. 521, 217(2004).
- [5] P. Spalart, "Direct simulation of a turbulent boundary layer up to $R_+ = 1410$," *J. Fluid Mech.*, vol 187, 61(1988).
- [6] G. Khujadze and M. Oberlack, "DNS and scaling laws from new symmetry groups of ZPG turbulent boundary layer flow," *Theoret. Comput. Fluid Dynamics*, vol. 18, 391(2004).
- [7] S. Hoyas and J. Jimenez, "Scaling of velocity fluctuations in turbulent channels up to $R_+ = 2000$," *Phys. of Fluids*, vol. 18, 011702(2006).
- [8] J. Komminaho and M. Skote, "Reynolds Stress Budgets in Couette and Boundary Layer Flows," *Flow, Turbulence and Combustion*, vol 68, 167(2002).
- [9] D. Weyburne, "A mathematical description of the fluid boundary layer." *Applied Mathematics and Computation*, vol. 175, 1675(2006). Also D. Weyburne, Erratum to "A mathematical description of the fluid boundary layer". *Applied Mathematics and Computation*, vol. 197, 466(2008).
- [10] D. Weyburne, "New Shape Parameters for the Laminar, Transitional, and Turbulent Velocity Profiles", US Air Force Tech Report AFRL-RY-HS-TR-2010-0016, 2010.
- [11] J. Lee and H. Sung, "Effects of an adverse pressure gradient on a turbulent boundary layer," *International Journal of Heat and Fluid Flow*, vol. 29, 568(2008).
- [12] M. Skote and D. Henningson, "Direct numerical simulation of a separated turbulent boundary layer," *J. Fluid Mech.*, vol. 471, 107(2002).
- [13] Y. Nagano, M. Tagawa and T. Tsuji, "Effects of Adverse Pressure Gradients on Mean Flows and Turbulence Statistics in a Boundary Layer," *Proc. 8th Symp. on Turbulent Shear Flows*, Springer-Verlag, pp 7-20, 1993.

- [14] P. Skåre and P. Krogstad, “A Turbulent Equilibrium Boundary Layer near Separation,” *J. Fluid Mech.*, vol. 272, 319(1994).
- [15] A. Cenedese, G. Romano, R. Antonia, “A comment on the “linear” law of the wall for fully developed turbulent channel flow”, *Experiments in Fluids*, vol. 25 165(1998).
- [16] J. Park and M. Chung, “Revisit of Viscous Sublayer Scaling Law”, *Phys. of Fluids*, vol. 16, 478(2004).
- [17] D. Poggi, A. Porporato, and L. Ridolfi, “An experimental contribution to near-wall measurements by means of a special laser Doppler anemometry technique”, *Experiments in Fluids*, vol. 32, 366(2002).
- [18] H. Nagib, C. Christophorou, and P. Monkewitz, “High Reynolds Number Turbulent Boundary Layers Subjected to Various Pressure-Gradient Conditions”, In: G. E. A. Meier and K. R. Sreenivasan (eds.) *One Hundred Years of Boundary Layer Research Proceedings of IUTAM Symposium* (pp. 383-394), Springer, Netherlands, 2006.
- [19] Schlichting, H., *Boundary Layer Theory*, 7th ed., McGraw-Hill, New York ,1979.

Appendix A

The following FORTRAN source code implements an approximate Musker velocity profile [3] for arbitrary values of k ($= \gamma$) and C for a given value of yp ($= y^+$):

```

* first define some often used constants
z1 = 1./3.
z2 = 2./3.
z3 = SQRT(3.)
z4 = SQRT(12.*C + 81.*k**3)
z5 = (2*C + 27*k**3 - 3*k**1.5*z4)**z1
z6 = (2*C + 27*k**3 + 3*k**1.5*z4)**z1
z7 = (2*C + 27*k**3 - 3*k**1.5*z4)**z2
z8 = (2*C + 27*k**3 + 3*k**1.5*z4)**z2
z9=1. + 3.*k*yp
*
u_m = (-2*z3*(-(2**z2*C*(z5 + z6)) - 9*2**z2*k**3*(z5 + z6) -
$ C**z1*z5*z6*(z5 + z6) + 2*2**z1*C**z2*(z7 + z8))*
$ ATAN((-2*2**z1*C**z1 + z5 + z6)/(z3*SQRT((z5 - z6)**2))) +
$ 2*z3*(-(2**z2*C*(z5 + z6)) - 9*2**z2*k**3*(z5 + z6) -
$ C**z1*z5*z6*(z5 + z6) + 2*2**z1*C**z2*(z7 + z8))*
$ ATAN((z5 + z6 - 2*2**z1*C**z1*z9)/(z3*SQRT((z5 - z6)**2))) +
$ SQRT((z5 - z6)**2)*(-2*C**z1*(2**z1*C**z1 + z5 + z6)**2 *
$ LOG(2**z1*C**z1 + z5 + z6) + (2**z2*C + 9*2**z2*k**3 +
$ 2*2**z1*C**z2*(z5 + z6) - C**z1*(2*z7 + z5*z6 + 2*z8))*
$ LOG(2**z2*C**z2 + z7 - 2**z1*C**z1*z6 + z8 -
$ z5*(2**z1*C**z1 + z6)) + 2*2**z2*C*LOG(z5 + z6 +
$ 2**z1*C**z1*z9) + 4*C**z2*(4*C + 54*k**3 -
$ 6*k**1.5*z4)**z1*LOG(z5 + z6 + 2**z1*C**z1*z9) +
$ 2*C**z1*z7*LOG(z5 + z6 + 2**z1*C**z1*z9) +
$ 4*C**z1*z5*z6*LOG(z5 + z6 + 2**z1*C**z1*z9) +
$ 2*C**z1*z8*LOG(z5 + z6 + 2**z1*C**z1*z9) + 4*C**z2*(4*C +
$ 54*k**3 + 6*k**1.5*z4)**z1*LOG(z5 + z6 + 2**z1*C**z1*z9) -
$ 2**z2*C*LOG(z7 - z5*z6 + z8 - 2**z1*C**z1*(z5 + z6)*z9 +
$ 2**z2*C**z2*z9**2) - 2*C**z2*(4*C + 54*k**3 - 6*k**1.5*z4)**z1*
$ LOG(z7 - z5*z6 + z8 - 2**z1*C**z1*(z5 + z6)*z9 +
$ 2**z2*C**z2*z9**2) + 2*C**z1*z7*LOG(z7 - z5*z6 + z8 -
$ 2**z1*C**z1*(z5 + z6)*z9 + 2**z2*C**z2*z9**2) +
$ C**z1*z5*z6*LOG(z7 - z5*z6 + z8 - 2**z1*C**z1*(z5 + z6)*z9 +
$ 2**z2*C**z2*z9**2) + 2*C**z1*z8*LOG(z7 - z5*z6 + z8 -
$ 2**z1*C**z1*(z5 + z6)*z9 + 2**z2*C**z2*z9**2) -
$ 2*C**z2*(4*C + 54*k**3 + 6*k**1.5*z4)**z1*LOG(z7 - z5*z6 +
$ z8 - 2**z1*C**z1*(z5 + z6)*z9 + 2**z2*C**z2*z9**2) -
$ 9*2**z2*k**3*LOG(((2**z1*C**z1 + z5 + z6)**2*(z7 - z5*z6 + z8 -
$ 2**z1*C**z1*(z5 + z6)*z9 + 2**z2*C**z2*z9**2)) / (z5 + z6 +

```

```

$ 2**z1*C**z1*z9)**2)))/(6.*C**z1*k*SQRT((z5 - z6)**2)*(z7 +
$ z5*z6 + z8))
*
      write(*,*)u_m,' = Musker velocity in plus units at yp given k and C '
*

```

The above approximate expression can be compared to the exact result obtained by the exact analytical integration (by Mathematica, software version 5.2) for specific values for k and C . Over the parameter range that we checked, $0.3 \leq k \leq 0.41$, $0.001 \leq C \leq 0.0025$, and $0 \leq yp \leq 30000$, the maximum difference between the exact integral expression and the above approximate integral expression is $\sim 7 \times 10^{-12}$. If the FORTAN compiler is forced to use double precision code, then for $yp=300$, $k=0.41$ and $C=0.001093$, the FORTRAN calculated velocity should be $u_m=18.920564156786$.